Advanced Powder Technology xxx (2011) xxx–xxx

Contents lists available at ScienceDirect

Advanced Powder Technology

journal homepage: www.elsevier.com/locate/apt

Original Research Paper

Decolorization of beads-milled TiO_2 nanoparticles suspension in an organic solvent

I Made Joni [a,b], Takashi Ogi [a], Agus Purwanto [c], Kikuo Okuyama [a,*], Terunobu Saitoh [d], Kazutaka Takeuchi [d]

[a] Department of Chemical Engineering, Graduate School of Engineering, Hiroshima University, 1-4-1 Kagamiyama, Higashi Hiroshima, Hiroshima 739-8527, Japan
[b] Department of Physics, Faculty of Mathematics and Natural Science, Padjadjaran University, Jl. Raya Bandung-Sumedang KM 21, Jatinangor 45363, Indonesia
[c] Department of Chemical Engineering, Faculty of Engineering, Sebelas Maret University, Jl. Ir. Sutami 36 A, Surakarta, Central Java 57126, Indonesia
[d] Material Processing Research Department 3, Canon Inc., 70-1, Yanagi-cho, Saiwai-ku, Kawasaki-shi, Kanagawa 212-8602, Japan

ARTICLE INFO

Article history:
Received 14 July 2010
Received in revised form 24 November 2010
Accepted 13 December 2010
Available online xxxx

Keywords:
TiO_2
Nanoparticle dispersion
Decolorization
Beads mill

ABSTRACT

In this paper, a new method is proposed for the decolorization of a yellow-hued suspension of rutile TiO_2 nanoparticles in an organic solvent (diethylene glycol dimethylether). The presence of color has always been undesirable in a suspension of nanoparticles filler used for industrial needs, particularly for optical applications.

A colorless suspension was achieved by irradiating well-dispersed TiO_2 nanoparticles in an organic solvent with UV-light (λ = 254 nm) for 5 h. TiO_2 nanoparticles of 1 and 5 wt.% were dispersed using a beads mill method. Trimethoxytrifluor(propyl) silane was used as a dispersant to achieve stability. The effect of the UV-light irradiation on the TiO_2 nanosuspension was investigated by means of a Fourier transform nuclear magnetic resonance analyzer (FT-NMR). The dispersant was partially desorbed due to the interaction of UV light and the TiO_2/dispersant complex. Thus, an enhanced transparency and the absence of color were obtained for well-dispersed TiO_2 nanoparticles in an organic solvent.

1. Introduction

Titanium dioxide (TiO_2) nanoparticles are known as useful filler for some composite materials — in particular, photosensitive materials such as photoanodes [1] and photocatalysts [2]. Due to a high refractive index [3], titanium dioxide (TiO_2) is used as nanocomposite filler in optical applications. The optical properties of TiO_2 nanocomposites depend on the content, size and size-distribution, and dispersion stability of the fillers. The dispersion of nanoparticles using a beads mill process was successfully achieved only after surface modification of the particles, as shown in our previous study [4,5]. Dispersion stability of nanoparticles in liquids is an important issue on various material properties and its applications [5–7]. The attractive forces between nanoparticles in a liquid suspension are sufficiently strong that nanoparticles tend to agglomerate in most monomers [8–12]. Our previous study successfully dispersed TiO_2 nanoparticles with a primary size of 15 nm in an organic solvent using a beads mill method and a dispersing agent to modify the surface of TiO_2 [4]. However, the color of well-dispersed TiO_2 nanoparticles in an organic solvent, i.e., diethylene glycol dimethyl ether (diglyme), was yellow. This suspension did not meet the application requirement as an alternative to glass, where a colorless and transparent performance is required. Therefore, for nanocomposite optical applications, a method that will produce a colorless dispersion of TiO_2 nanoparticles in an organic solvent becomes important. In the present study, a fluorinated compound (trimethoxytrifluor(propyl) silane) ($CF_3CH_2CH_2Si(OCH_3)_3$) was applied as a dispersing agent and ultraviolet (UV) irradiation was applied to obtain a color degradation of dispersed TiO_2 nanoparticles in an organic solvent — a method that has never been investigated.

TiO_2 particles tend to absorb UV light due to a high intrinsic band gap (3.0 eV for rutile). UV light excites the electrons from the valence and conduction bands of TiO_2, leaving holes in the valence band. These electrons and holes can initiate a redox reaction with the molecular species adsorbed onto the surfaces of TiO_2 particles. Anpo and Takeuchi [13] reported that UV-light irradiation of a TiO_2 catalyst generates electron–hole pairs, which can be represented as a localized electron (Ti^{3+}) and a hole (O^-(lattice)) and/or OH radicals. Some of these electron–hole pairs disappeared after recombination on bulk TiO_2, while other electrons and holes diffused to the surface of the TiO_2 to react with various hydrocarbons (i.e., hydrogenolysis and the formation of oxygen-containing organic compounds). Thus, due to the photocatalytic activities of the TiO_2 particles, it is reasonable to apply UV irradiation to a solution to obtain the color degradation of dispersed TiO_2 nanoparticles in an organic solvent.

A Fourier transform nuclear magnetic resonance analyzer (FT-NMR) was used to measure the effect of UV irradiation exposure on the adsorbed dispersant on TiO_2 particles. Furthermore, the

* Corresponding author. Tel.: +81 82 424 7716; fax: +81 82 424 5494.
E-mail address: Okuyama@hiroshima-u.ac.jp (K. Okuyama).

0921-8831/$ - see front matter © 2010 The Society of Powder Technology Japan. Published by Elsevier B.V. and The Society of Powder Technology Japan. All rights reserved.
doi:10.1016/j.apt.2010.12.008

effects of UV irradiation exposure on the dispersion properties of TiO_2 nanoparticles were evaluated with respect to their dispersion stability, particle size distribution, and optical transparency.

2. Experimental section

2.1. Beads mill process

Commercially produced TiO_2 nanoparticles with unmodified surface particles and a primary particle diameter of 15 nm (MT150A, rutile phase; Tayca Co., Ltd., Japan) were used in the present study. A silane coupling agent (SCA), trimethoxytrifluor(propyl) silane (Shin Etsu, Kagaku Co., Ltd., Japan), was used as a dispersing agent to alter the surface of TiO_2 nanoparticles. The typical structure of this SCA is $(XO)_3SiCH_2CH_2$-R, where XO is a hydrolyzable group ($X = CH_3$) and R is an organofunctional group ($R = CF_3$). The SCA content in the suspension was twice the TiO_2 content — i.e., 2 wt.% for SCA compared with 1 wt.% for TiO_2 nanoparticles.

A detailed description of the beads mill equipment has been reported previously [8,9]. Briefly, the beads mill (Kotobuki Industries Co., Ltd., Japan) was composed of a 170 mL vessel, a pump, and a mixing tank, as shown in Fig. 1. The beads mill contained 30 μm ZrO_2 (zirconia) beads (Neturen Co., Ltd., Tokyo, Japan). Nanoparticles were dispersed in an organic solvent of diethylene glycol dimethylether ($(CH_3OCH_2CH_2\text{-})_2O$) (Kishida, Kagaku Co., Ltd., Japan). The vessel was filled with beads to 70% capacity. The TiO_2 particle suspension was pumped into the vessel, which contained zirconia beads and a centrifugation rotor operated at a speed of 73.8 Hz (6095 rpm). The beads were agitated in the lower portion of the vessel (dispersing section) to break up the aggregate to avoid agglomeration of TiO_2 nanoparticles in the suspension. After dispersion, the suspension was pumped from the dispersing section to the upper region (separation section) where centrifugal force was used to separate the zirconia beads from the particle suspension. Centrifugal forces for beads separation in the upper part of the vessel were generated by rotating the outer cylindrical wall. The TiO_2 particle suspension was then recycled back to the dispersing section. In order to keep the temperature of the system constant, the vessel was supported by a water jacket system and was completely sealed. Suspensions of TiO_2 particles in diglyme with two TiO_2 concentrations, i.e., 1 or 5 wt.%, were pumped through the beads mill at an optimized recirculation mass flow rate of 20.3 kg/h. The well-dispersed suspension then was illuminated under UV irradiation ($\lambda = 254$ nm) (30 W, DM-90, Dishin Co., Ltd., Japan) for 5 h to obtain a colorless suspension of rutile TiO_2 particles in diglyme.

2.2. Characterization

Particle size distribution of the TiO_2 suspension at the selected time was measured using dynamic light scattering with a HPPS-5001 Malvern Instrument. Field emission scanning electron microscopy (FE-SEM, S-5000, Hitachi Ltd., Tokyo, Japan) was used to observe the morphology of the TiO_2 dispersion inside the organic solvent before and after beads milling. The morphology of the particles was also examined visually using transmission electron microscopy (TEM, JEM-3000F Japan Electron Optics Laboratory Ltd., Tokyo, Japan). The optical transmission properties of the suspensions were measured by UV–vis spectroscopy (U-2810, Hitachi, Japan) at different TiO_2 concentrations.

The state of the surface alteration following UV irradiation for 5 h on a rutile TiO_2 particle suspension was investigated using a Fourier transform nuclear magnetic resonance analyzer (FT-NMR) (JEOL ECA-500, USA). ^{19}F NMR and ^{1}H NMR spectral measurements were used to investigate the state of the organofunctional ($R = CH_3$) and hydrozable groups ($X = CF_3$) in trimethoxytrifluor(propyl) silane, respectively. The ^{19}F NMR operated at a magnetic field strength of 11.747 T at 470 MHz in a measurement range of −200 ppm to 0 ppm. Fluorine chemical shifts (^{19}F δ, ppm) were given relative to TFA (trifluoroacetic acid) as a standard. The fluorine chemical shifts were determined by using 32,768 points in the time domain. The ^{1}H NMR was operated at a magnetic field strength of 11.747 T at 500 MHz in a measurement range of −3 ppm to 15 ppm. Proton chemical shifts (^{1}H δ, ppm) were given relative to TMS (tetra methyl silane) as a standard. The proton chemical shifts were determined by using 16,384 points in the

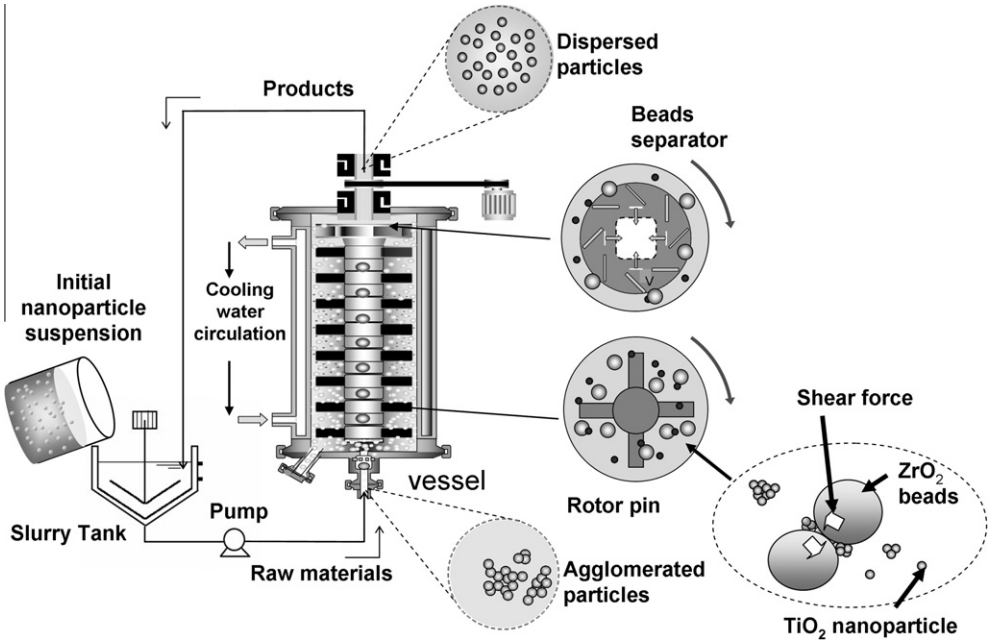

Fig. 1. The beads mill instrument and dispersion mechanism of nanoparticles.

Please cite this article in press as: I.M. Joni et al., Decolorization of beads-milled TiO_2 nanoparticles suspension in an organic solvent, Advanced Powder Technology (2011), doi:10.1016/j.apt.2010.12.008

time domain. A deuterated chloroform was used as a solvent for both ^{19}F and ^{1}H NMR, and was operated at room temperature.

3. Results and discussion

3.1. Evolution of particle size and morphology

Physical methods for particle dispersion such as beads mill often caused a change in particle morphology due to mechanical milling of the particles. Fig. 2a shows a SEM image of the initial rutile TiO_2 nanoparticles before the beads milling process. The morphology of an initial rutile TiO_2 was that of an agglomerated rod-shape. The primary average diameter and length of the rod-shape of the initial rutile TiO_2 was 15.5 and 109 nm, respectively. The TiO_2 nanoparticle suspension in organic solvent was agglomerated with a size of around 1–10 μm as shown in Fig. 2b. This result shows that the dispersion of nanoparticles in an organic solvent was difficult without a dispersing agent. Fig. 2c shows a SEM image of the rutile TiO_2 nanoparticles after the beads milling process. The primary particles appeared to have undergone a morphology change from rod-shaped to more spherical following the beads milling process. This result was in agreement with a previous investigation, as reported in Ref. [4]. The average size (D_{50}) of particles after beads milling was 30 nm, as shown in Fig. 2c. This result indicated that the shear force between beads rotated at 6095 rpm in the dispersing section enhanced the size reduction of the agglomerated particles and changed the shape of the TiO_2 particles.

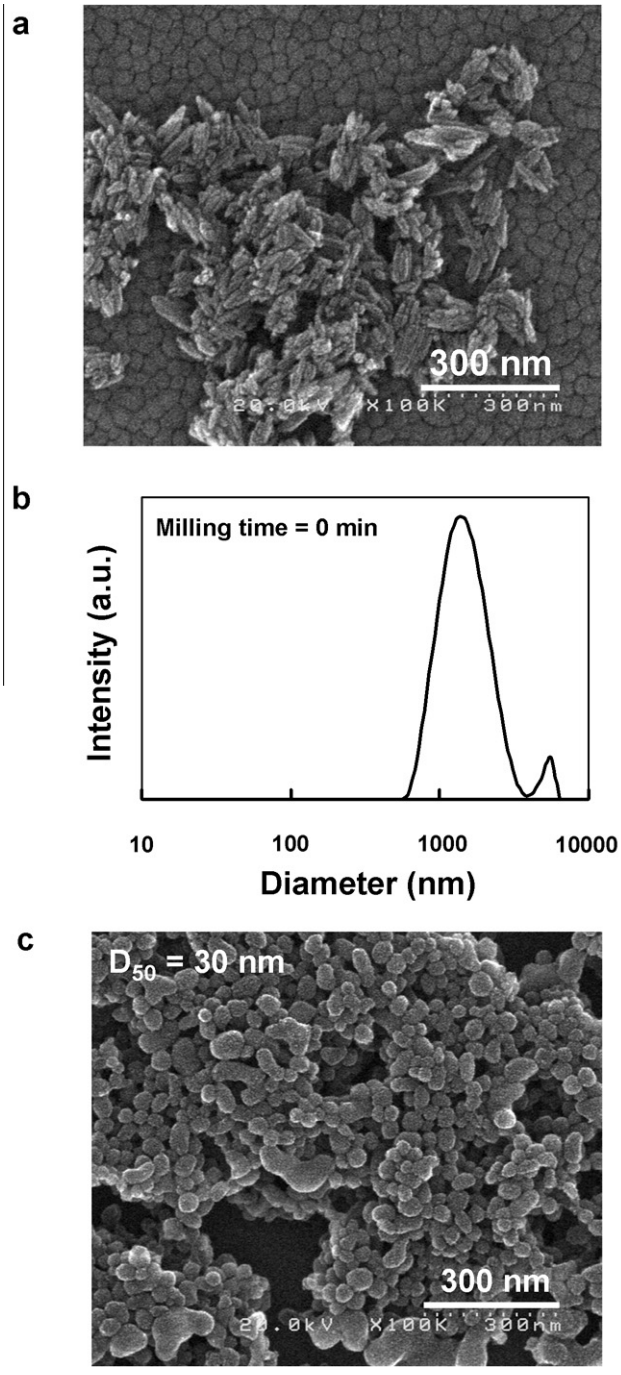

Fig. 2. (a) The morphology of TiO_2 nanoparticles by SEM measurement before beads milling, (b) particles size distribution of TiO_2 suspension before beads milling, and (c) the morphology of TiO_2 nanoparticles by SEM measurement after beads milling.

Fig. 3 shows the TEM images of the morphology of the rutile TiO_2 particle suspension in diglyme before and after the beads milling process. The TEM image of the initial rutile TiO_2 nanoparticles before beads milling was rod-shaped (Fig. 3a). The TEM images in Fig. 3b also show that particles appear to have undergone a morphology change from rod-shaped to more spherical following beads milling. This result shows that the TEM images were identical with the SEM results as shown in Figs. 2a and c.

3.2. TiO_2 particle dispersion characteristics

Suspension of particles prepared via mechanical disruption using a beads milling process, without a dispersing agent, often caused re-aggregation of particles when the mechanical disrupting action was stopped. Thus, in order to increase the stability of the suspension, a dispersing agent of a silane-based trimethoxytrifluor(propyl) silane was used as a dispersing agent. Figs. 4a and b show the visual image of the suspension and changes in size distribution of a 1 wt.% rutile TiO_2 nanoparticle dispersed in organic solvent at different milling times, respectively. With a milling time in the range of 0–180 min, the TiO_2 suspension was agglomerated and formed sediment, as shown in Fig. 4a. Because of the particle agglomeration, particle size grew to beyond the size limit, which caused particles to sink simply from the dominant force of gravitation. However, around 285 min, particles were well-dispersed with an average size of 15.8 nm, as confirmed by Fig. 4b, which shows that the main peak of the size distributions were shifted smaller as milling times increased. The particle size distribution within a milling time range of 60–120 min indicated that the suspension was unstable. At a milling time of 180 min, the main peak of the size distribution shifted almost to the primary size, which showed successful achievement in size reduction. However, particles started to re-agglomerate, as shown in Fig. 4b (225 min), which indicated that the suspension was unstable. The surface alteration of the TiO_2 particles, using trimethoxytrifluor(propyl) silane, successfully attained well-dispersed TiO_2 particles in organic solvent after a milling time of 285 min. The beads milling achieved dispersed particles with an average size of 15.8 nm, which was close to the primary size of TiO_2 particles. As previously reported in Ref. [4], surface alteration of TiO_2 particles enabled the particle surfaces to avoid close contact with a number of forces, including electrostatic attraction, covalent bonding, hydrogen bonding, and solvation of various species. Various mechanisms of these forces and their effect on the electrical double layer have been reported [4,9] and described elsewhere [14–18]. Briefly, a dispersing agent may have promoted the formation of a very stable siloxane bond on the particle surfaces [4,15] (Si–O–Si) and improved the steric barrier at the double layer. The modified surface of TiO_2 particles was able to overcome interparticle interaction energy due to Van

Please cite this article in press as: I.M. Joni et al., Decolorization of beads-milled TiO_2 nanoparticles suspension in an organic solvent, Advanced Powder Technology (2011), doi:10.1016/j.apt.2010.12.008

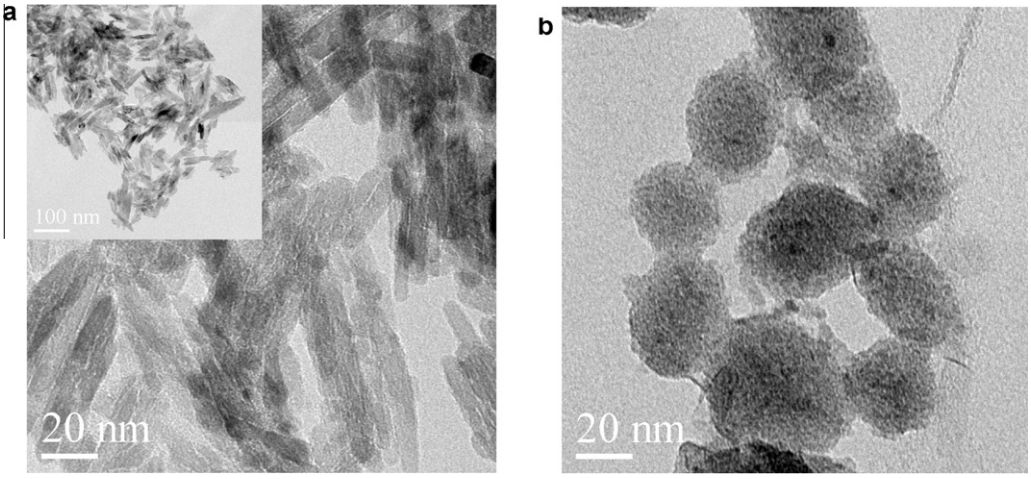

Fig. 3. The morphology of TiO_2 nanoparticles by TEM measurement (a) before and (b) after beads milling.

der Waals forces, which reduced the shear rate to the lowest state to bring the shear stress equal to the yield value [16–18] and to promote better dispersion in each cycle of the beads milling process [4].

3.3. Effect of UV-light irradiation on the microstructure of the TiO_2 surface

Although the beads-milled TiO_2 nanoparticles were well-dispersed in an organic solvent, the color of the solution was yellow. The suspension was illuminated under UV irradiation ($\lambda = 254$ nm) for 5 h to obtain a colorless suspension of rutile TiO_2 particles in diglyme. Furthermore, ^{19}F NMR and ^{l}H NMR spectral measurement was obtained from the suspension before and after UV irradiation to investigate its effect. Figs. 5a and b show the ^{19}F NMR spectral measurements of the yellow TiO_2 dispersion (before UV irradiation) and measurement of a transparent solution (after UV irradiation), respectively. The horizontal axis and vertical axis indicated the chemical shift (δ) and the peak intensity, respectively. The peak area or integrated curve given near the NMR peak was proportional to the number of *F* or fluorine of the sample under investigation. The resonance frequencies of different chemical groups differ due to the different magnetic shielding caused by surrounding electrons. This difference was presented as a chemical shift given in ppm compared to a reference — in the case of ^{19}F NMR, the TFA (trifluoroacetic acid) was used as the reference. The ^{19}F NMR spectra in Fig. 5a shows a single peak that indicated the presence of trifluoromethyl ($X = CF_3$) of the trimethoxytrifluor(propyl) silane (structure $X\text{-}CH_2CH_2Si(O\text{-}R)_3$) in suspension. The ^{19}F chemical shift of CF_3 in trimethoxytrifluor(propyl) silane was −70 ppm. A comparison between Figs. 5a and b show that there was no change in the ^{19}F chemical shift of CF_3 and the peak area after UV irradiation. This result suggested that the organofunctional part of the fluorinated compound was stable under UV irradiation.

An ^{l}H NMR spectra of the suspension was obtained to examine the state of the hydrolyzable group ($R = CH_3$) in trimethoxytrifluor (propyl) silane ($X\text{-}CH_2CH_2Si(O\text{-}R)_3$) and the state of solvent of diethylene glycol dimethylether or $(CH_3OCH_2CH_2\text{-})_2O$ after UV irradiation. Figs. 6a and b show the ^{l}H NMR spectra of the suspension before and after UV irradiation, respectively. Similar to the ^{19}F NMR, the peak area given near the ^{1}H NMR peak was proportional to the number of H or protons of the sample under investigation. The notations that represent the diglyme and SCA structure with their corresponding ^{1}H NMR spectra appearing in Figs. 6a and b are described in Figs. 7a and b, respectively. Fig. 7a shows the chemical structure of the solvent and its corresponding notation of ^{1}H NMR peaks ($^{a}CH_3$, $^{b}CH_2$ and $^{c}CH_2$). Fig. 7b shows the chemical structure of the dispersing agent and its corresponding ^{1}H NMR peaks ($^{d}CH_2$, $^{e}CH_2$, and $^{f}CH_3$).

The ^{1}H signals of the diglyme appeared in an ^{1}H chemical shift range of 3.7–3.2 ppm compared to the TMS (tetra methyl silane) as standard (Fig. 6a). The ^{1}H chemical shifts of the diglyme were 3.38, 3.52 and 3.6 ppm for $^{a}CH_3$, $^{b}CH_2$ and $^{c}CH_2$, respectively. The peak areas of the ^{1}H signal in the diglyme were 6, 3.94 and 4.598 for corresponding chemical groups of $^{a}CH_3$, $^{b}CH_2$, and $^{c}CH_2$, respectively. These peak areas were proportional to the number of H or protons on each corresponding chemical group in diglyme. Neither the chemical shifts nor the peak areas appeared to change after UV irradiation according to the ^{1}H NMR signals of the diglyme, as shown in Fig. 6b. This result suggested that there was no decomposition of the solvent after UV irradiation.

The peak area of the $^{e}CH_2$ increased nearly twice and also a new ^{1}H signal peak appeared, as shown in ^{g}OH. The ratio of the peak area of $^{a}CH_3$ and $^{e}CH_2$ in Fig. 6b increased compared to the ratio of the peak area in Fig. 6a. This increase in the ratio of the peak area indicated that the SCA in the surface of TiO_2 particles was partially desorpted due to the photoreactive properties of TiO_2 under UV-light irradiation. The peak (d) was not clear due to the appearance of a small signal compared with the large solvent signals. The peak of f also was too small because the $^{f}CH_3$ reacted with the TiO_2 surface after the beads mill process.

The desorption of the silane coupling agent from the surface of TiO_2 due to interaction between UV light and TiO_2/surfactant can be explained as follows. The absorption of TiO_2 under UV-light irradiation promoted electrons from the valence band of TiO_2 into the conduction band, leaving behind a positively charged species, or hole, in the valence band [19–21]. Photoirradiation of a TiO_2 nanoparticle dispersion, with photon energies larger than the bandgap (3 eV), created electron–hole (e^-/h^+) pairs, as follows:

$$TiO_2 + UV \rightarrow e^-_{cb}(TiO_2) + h^+_{vb}(TiO_2) \quad (1)$$

where e^-_{cb} and h^+_{vb} were electrons in the conduction and holes in the valence band, respectively. Consequently, following irradiation, the TiO_2 nanoparticles acted as either electron or hole donors to reduce oxidized materials in the TiO_2 surface [22–24].

The electrons and holes that participated in the oxidation/reduction reactions with adsorbed molecules on the TiO_2 surface caused a color change from a yellow hue to a colorless solution [13,14]. The color of a composite material was a complex

Please cite this article in press as: I.M. Joni et al., Decolorization of beads-milled TiO_2 nanoparticles suspension in an organic solvent, Advanced Powder Technology (2011), doi:10.1016/j.apt.2010.12.008

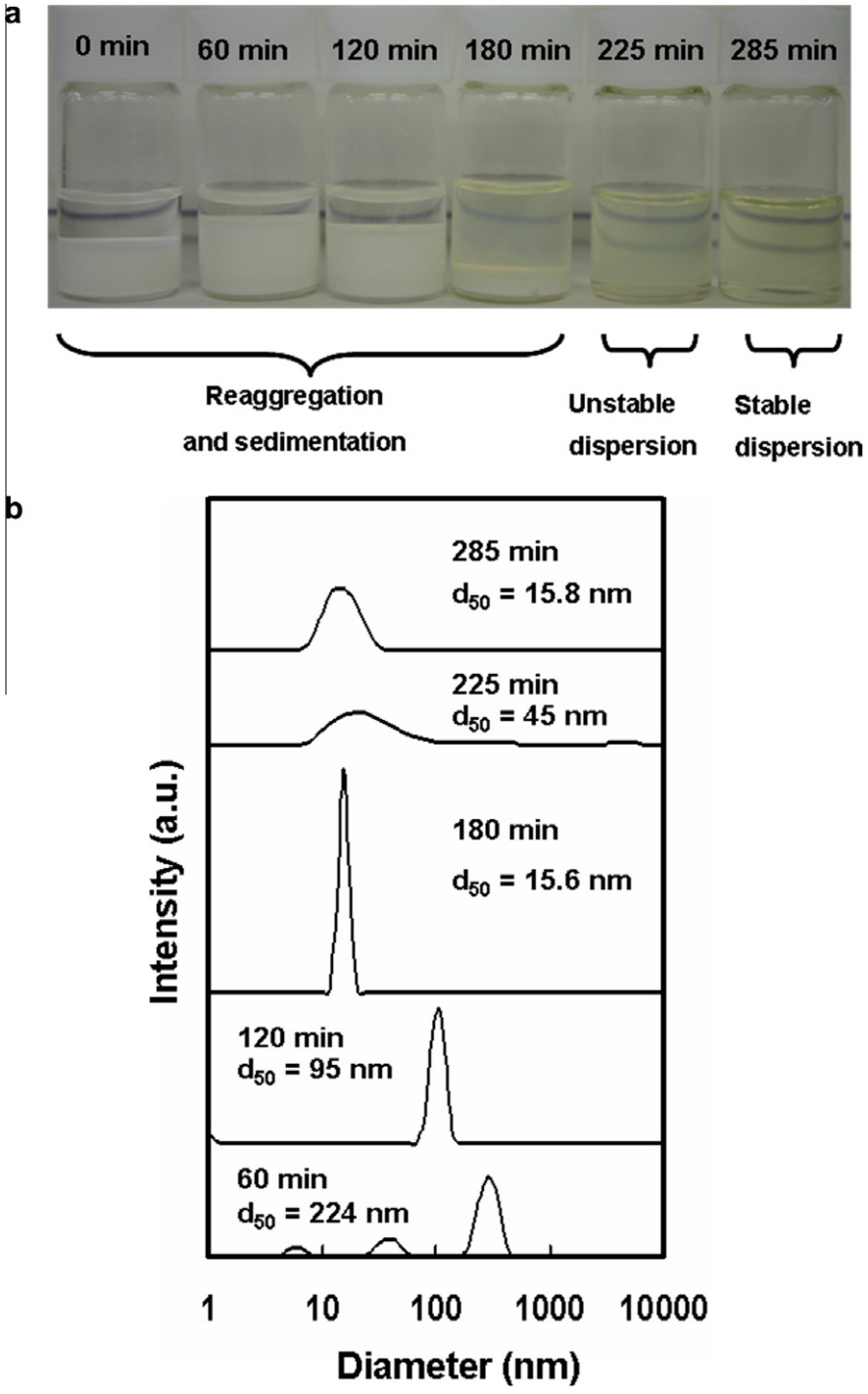

Fig. 4. The beads-milled TiO_2 nanoparticles of 1 wt.% in diglyme: (a) the visual image of the suspension stability and (b) the particle size distribution of the suspension at different milling times.

combination of optical behaviors within the material. This result suggested that the decolorization of well-dispersed TiO_2 nanoparticles in organic solvent was due to the decomposition of the organofunctional part of SCA and following desorption of the SCA from the surface of TiO_2 nanoparticles. When a white incident light transmits through the material, the light would be scattered by surface-modified fine-size TiO_2 particles within the material before it emerges and reaches the eye of the observer with the specific optical and color information of the material or suspension.

Furthermore, the dispersion of rutile TiO_2 nanoparticles using a fluorinated compound as a dispersant was repeated for higher TiO_2 content (5 wt.%). Fig. 8 shows the effect of UV irradiation for about 5 h on the size distribution of dispersed TiO_2 particles at different TiO_2 particle contents, i.e., 1 and 5 wt.%. At the lower TiO_2 content (1 wt.%), the main peak of particle size distribution did not change position and two new peaks at ~600 and ~6000 nm appeared. Thus, the average size of TiO_2 particles changed from 15.6 to 255 nm. A high intensity of the UV light received by TiO_2 particles in a low particle concentration caused the increase in particle size due to re-agglomeration of some TiO_2 particles in suspension. However, for a higher TiO_2 content (5 wt.%), the particle size distribution was relatively mono dispersed, and the average size was

Please cite this article in press as: I.M. Joni et al., Decolorization of beads-milled TiO_2 nanoparticles suspension in an organic solvent, Advanced Powder Technology (2011), doi:10.1016/j.apt.2010.12.008

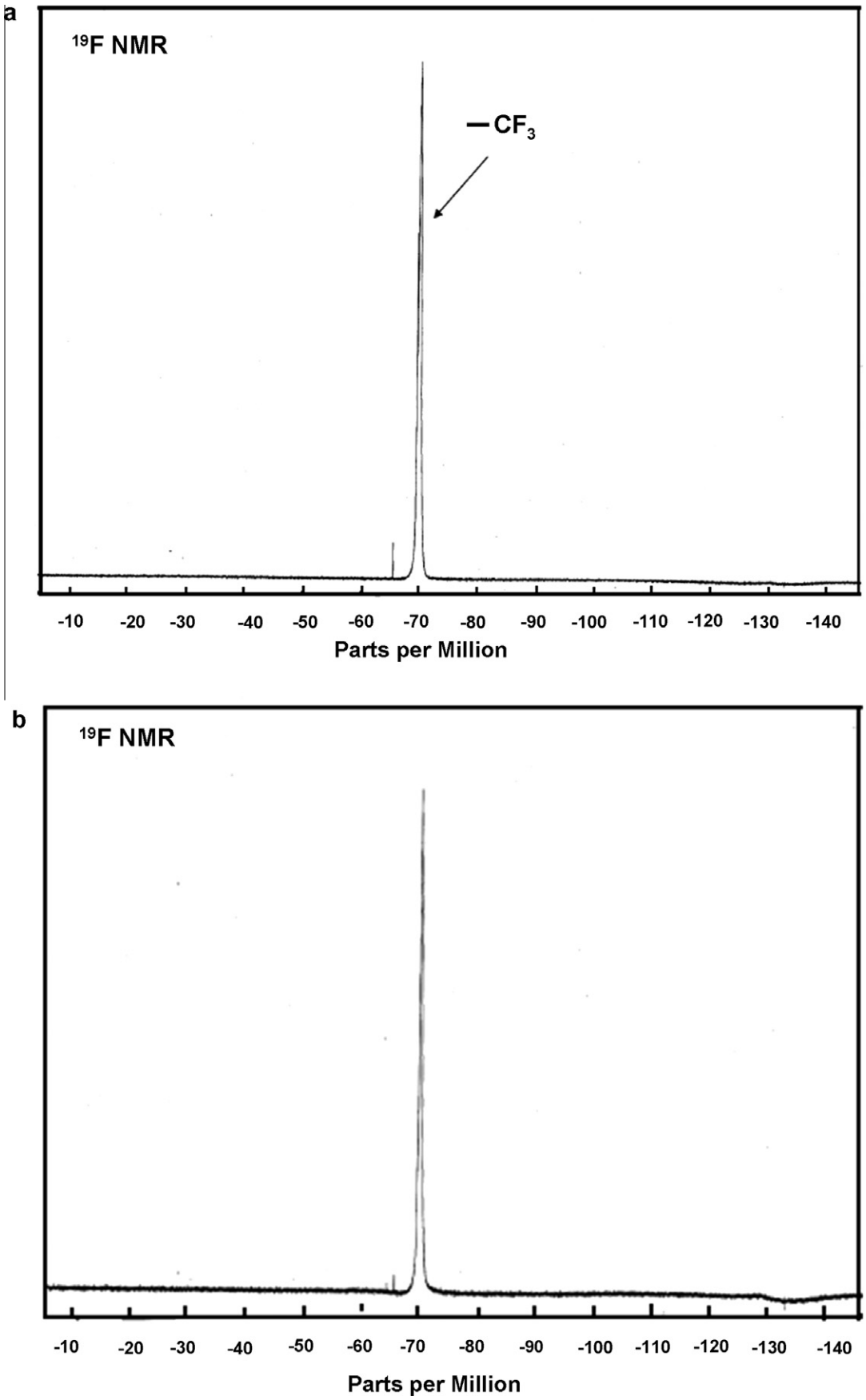

Fig. 5. The ^{19}F-NMR spectra of well-dispersed TiO_2 nanoparticles in diglyme: (a) before UV irradiation and (b) after UV irradiation.

Please cite this article in press as: I.M. Joni et al., Decolorization of beads-milled TiO_2 nanoparticles suspension in an organic solvent, Advanced Powder Technology (2011), doi:10.1016/j.apt.2010.12.008

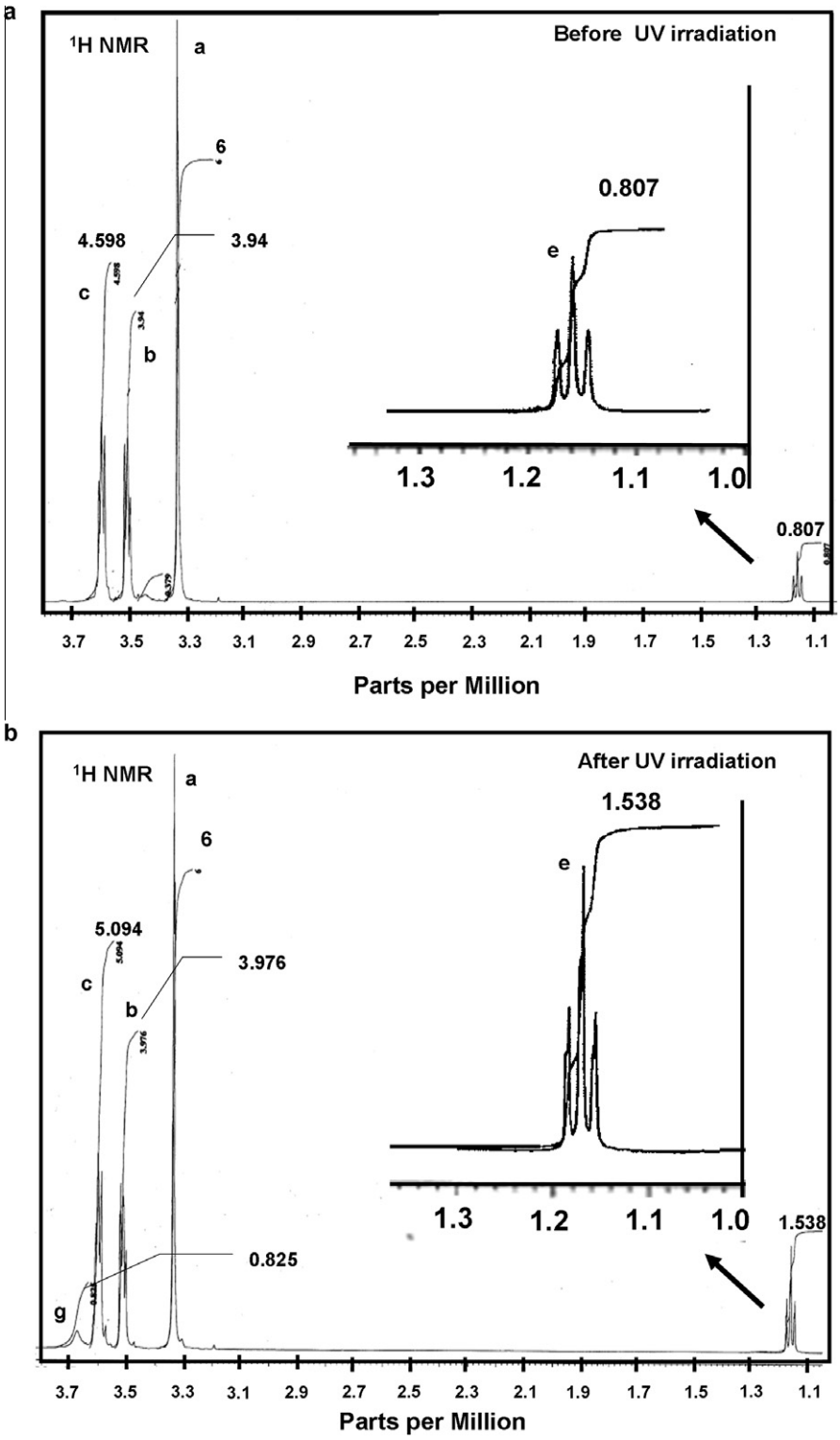

Fig. 6. The ^{1}H-NMR spectra of well-dispersed TiO_2 nanoparticles in diglyme: (a) before UV irradiation and (b) after UV irradiation.

slightly changed from 19.9 to 20.3 nm. The change in the particle size distribution may be because UV irradiation had slightly changed the stability of the suspension. However, the increase in particle size due to agglomeration did not exceed the size limit that caused particles to sink simply from gravitation. Thus, the dispersion of particles did not create sedimentation.

Fig. 9a shows the transmittance properties of dispersed TiO_2 nanoparticles at 1 wt.% both before and after UV irradiation, and Fig. 9b shows a comparison of the transmittance properties at different TiO_2 contents (1 and 5 wt.%). Exposure of the dispersed TiO_2 of 1 wt.% with a UV irradiation for 5 h caused the surface of particles to undergo surface alteration, as indicated by the changing of

Please cite this article in press as: I.M. Joni et al., Decolorization of beads-milled TiO_2 nanoparticles suspension in an organic solvent, Advanced Powder Technology (2011), doi:10.1016/j.apt.2010.12.008

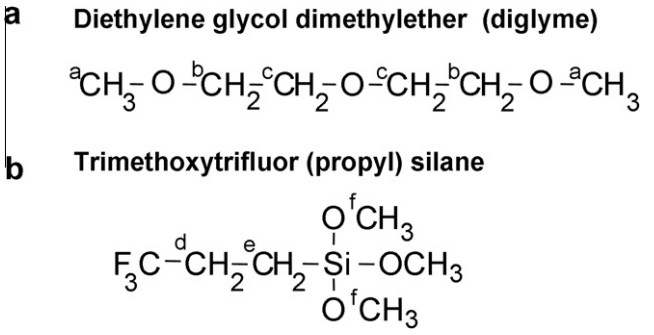

Fig. 7. The chemical structure and its corresponding notations on the ^{1}H-NMR spectra: (a) organic solvent and (b) dispersing agent.

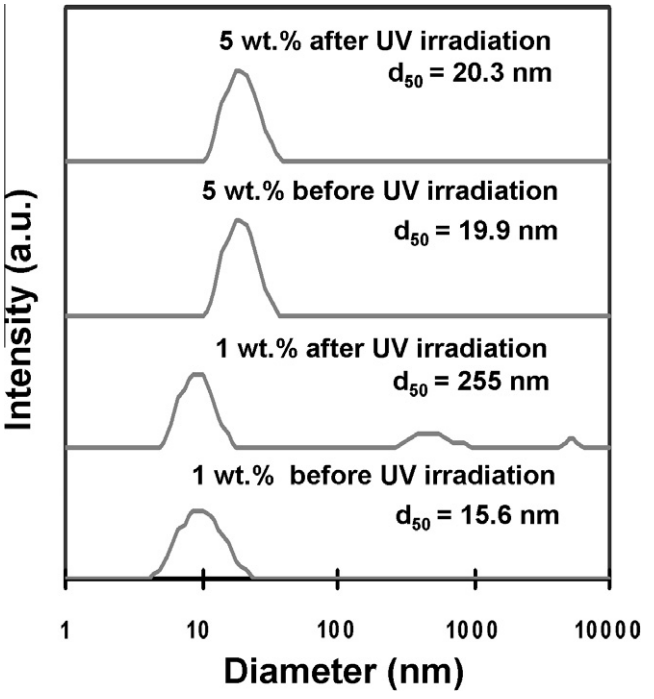

Fig. 8. The size distribution of well-dispersed TiO_2 nanoparticles in diglyme before and after UV irradiation at 1 and 5 wt.% of TiO_2 content. The D_{50} is the mean size of particles measured using HPPS-5001 Malvern Instrument.

the solution color from yellow (Fig. 9a(1)) to colorless and transparent (Fig. 9a(2)). According to the Rayleigh scattering law formula Eq. (2), the optical transparency loss of the suspension depends on the average size of the particles, volume fraction, refractive index of the particles and matrix [25,26].

$$T = \frac{I}{I_0} = \exp\left(-\frac{32\pi^4\phi_V l\, r^3 n_m^4}{\lambda^4}\left[\frac{(n_p/n_m)^2-1}{(n_p/n_m)^2+2}\right]^2\right) \quad (2)$$

This formula is a transparency loss (T) of the nanocomposite as a result of light scattering when the nanocomposite consists of randomly dispersed spherical particles with radius (r) and particles volume fraction (ϕ_V); where I and I_0 are the intensities of the transmitted and incident light, respectively, λ is the wavelength of the light, l is the optical path length, and n_p and n_m are the refractive index of the particles and the matrix, respectively. To avoid the effect of particle size on the transparency loss, particle size reduction has to be significantly below the visible light. The optical scattering loss can be avoided when the particle mean size is less than one-tenth of the visible light wavelength (200–800 nm) or typically

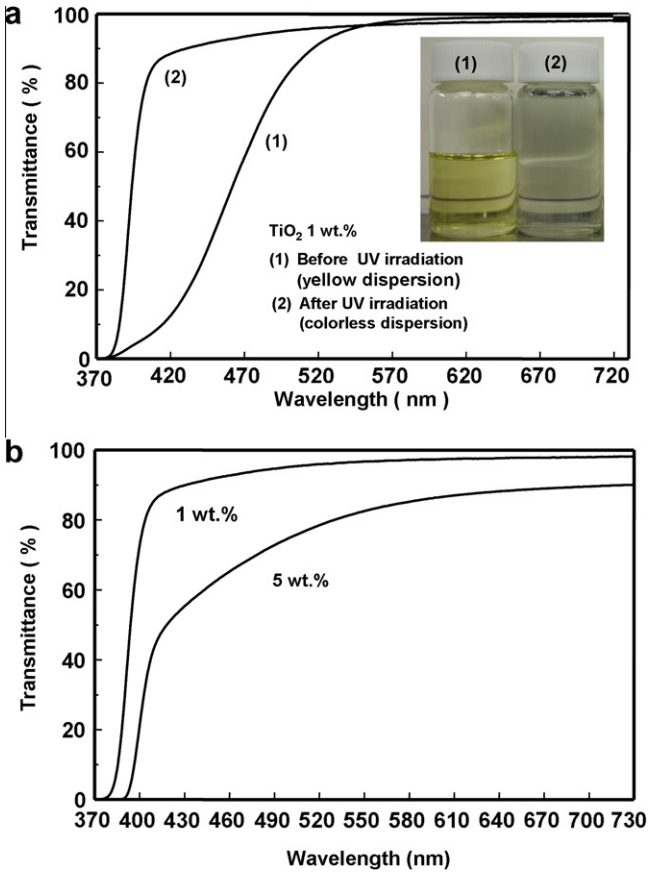

Fig. 9. Transmittance properties of well-dispersed TiO_2 nanoparticles in diglyme: (a) before and after UV irradiation and (b) after UV irradiation with a different TiO_2 content.

<25 nm [26]. On the control of particles size, as shown in Fig. 4b, suspension of TiO_2 particles in diglyme under well-dispersed conditions resulted in a particle size below 25 nm. Thus, the contribution of the particle size on the light scattering loss can be neglected. Consequently, the main factor that contributed to the strong light scattering loss of suspension was the refractive index of the particles and the matrix. The desorption of the surfactant was suggested to be the main factor causing a change in the refractive index of the matrix (n_m) due to an excess of surfactant in the organic solvent. The UV irradiation of the suspension utilized the matching of the refractive index of particles and organic solvent. Finally, the optical scattering loss could be avoided, and the as-prepared suspension achieved enhanced transparency.

Fig. 9b shows the optical transparency of the suspension with differing TiO_2 nanoparticle contents of 1 and 5 wt.%. Although the suspension had a high TiO_2 content, the effect of UV irradiation on color degradation was similar, and the color of the solution was changed from yellow to colorless with an enhanced transparency. By contrast, with a lower TiO_2 content (1 wt.%), the solution achieved an enhanced transparency of more than 90%. The transparency of a higher TiO_2 content (5 wt.%) was approximately 80%. Nevertheless, the range of enhanced transparency of an as-prepared TiO_2 nanoparticle dispersion in diglyme had met the requirement for optical applications.

The color of colloidal gold depends on both the size and shape of the particles, as well as the refractive index of the surrounding medium [27,28]. Mie calculations by Creighton and Eadon have indicated that for the majority of metals, surface plasmon absorption contributes significantly to the UV–visible spectrum [29].

Please cite this article in press as: I.M. Joni et al., Decolorization of beads-milled TiO_2 nanoparticles suspension in an organic solvent, Advanced Powder Technology (2011), doi:10.1016/j.apt.2010.12.008

Adsorption of silane may have changed the electrochemical on the surface of nanosized TiO_2 particles resulted in yellow hued TiO_2 suspension. The desorption of silane possibly changed both the refractive index of the particles and solvent. The change on the color of nanoparticles suspension may be caused by the change of the solvent refractive index, according to the Mie theory [27,30], and also possibly by the surface alteration due to desorption [31]. However, further investigation is necessary to know how the adsorption and desorption of silane change the surface plasmon absorption and lead to its contribution on the color of the suspension.

4. Conclusions

In the present study, the UV-light irradiation method used on well-dispersed TiO_2 nanoparticles in an organic solvent successfully achieved a colorless and enhanced transparency. The surface state of TiO_2 particles influenced the transparency and color properties of suspension. The UV-light irradiation of well-dispersed TiO_2 particles in an organic solvent decomposed the hydrozable part of the silane coupling agent in the surface of TiO_2 particles. Thus, the desorption of the silane coupling agent from the surface of TiO_2 was considered to be the main factor for the change of the color and transparency of the suspension. The selection of the dispersing agent was crucial both for dispersion stability and the optical properties of the TiO_2 nanoparticle dispersion in an organic solvent. In addition, the UV-light irradiation on the suspension did not change the stability of the suspension for the TiO_2 content in the suspension was 5 wt.% and slightly changed for the TiO_2 content in the suspension was 1 wt.%. However, UV irradiation on the suspension for the TiO_2 content 5 wt.% or less than 5 wt.% have resulted a decolorization and lead the suspension to be transparent. The dispersion of TiO_2 by beads mill process was difficult for higher TiO_2 content since the slurry of the suspension in the TiO_2 content higher than 5 wt.% was in very high viscosity. Further investigation is necessary to improve the dispersion of high TiO_2 nanaparticles content in suspension and to know in what extent the UV irradiation could lead to decolorization of the suspension.

Acknowledgment

The authors thank Dr. Eishi Tanabe from Western Hiroshima Prefecture Industrial Research Institute, for the TEM measurement. We also thank Mr. Takuya Nishiwaki for his assistance with the experiment. The work was supported by a Grant-in-Aid for Scientific Research A (No. 22246099). We acknowledge the Ministry of National Education of the Republic of Indonesia for providing a doctoral scholarship (I.M.J).

References

[1] J. Byrne, E. Anthony, R. Brian, Photoelectrochemistry of oxalate on particulate TiO_2 electrodes, J. Electroanal. Chem. 457 (1998) 61–72.
[2] H. Yoneyama, T. Torimoto, Titanium dioxide/adsorbent hybrid photocatalysts for photodestruction of organic substances of dilute concentrations, Catal. Today 58 (2000) 133–140.
[3] M. Inkyo, Y. Tokunaga, T. Tahara, T. Iwaki, F. Iskandar, C.J. Hogan, K. Okuyama, Beads mill-assisted synthesis of poly methyl methacrylate (PMMA)-TiO_2 nanoparticles composites, Ind. Eng. Chem. Res. 47 (2008) 2597–2604.
[4] I.M. Joni, A. Purwanto, F. Iskandar, K. Okuyama, Dispersion stability enhancement of titania nanoparticles in organic solvent using a bead mill process, Ind. Eng. Chem. Res. 48 (2009) 6916–6922.
[5] M. Takeda, E. Tanabe, T. Iwaki, A. Yabuki, K. Okuyama, Importance of dispersibility of TiO_2 in preparation of TiO_2-dispersed microspheres by Shirasu porous glass (SPG) membrane emulsification, Adv. Powder Technol. 20 (2009) 361–365.
[6] E. Baez, N. Quazi, I. Ivanov, S.N. Bhattacharya, Stability study of nanopigment dispersions, Adv. Powder Technol. 20 (2009) 267–272.
[7] K. Cho, Y.J. Suh, H. Chang, D.S. Kil, B.G. Kim, H.D. Jang, Synthesis of mesoporous $CaCO_3$ particles by a spray drying method from the stable suspensions achieved in a beads mill, Adv. Powder Technol. 21 (2010) 145–149.
[8] M. Inkyo, T. Tahara, Dispersion of agglomerated nanoparticles by micromedia mill, Ultra Apex Mill, J. Soc. Powder Technol. Jpn. 41 (2004) 578–589.
[9] M. Inkyo, T. Tahara, T. Iwaki, F. Iskandar, C.J. Hogen, K. Okuyama, Experimental investigation of nanoparticles dispersion by beads milling with centrifugal bead separation, J. Colloid Interf. Sci. 304 (2006) 535–540.
[10] E.S. Lee, S.M. Lee, W.R. Cannon, D.J. Shanefield, Improved dispersion of aluminum nitride particles in epoxy resin by adsorption of two-layer surfactants, Colloids Surf. A 316 (2008) 95–103.
[11] A. Reindl, A. Voronov, P.K. Gorle, M. Rauscher, A. Roosen, W. Peukert, Dispersing and stabilizing silicon nanoparticles in a low-epsilon medium, Colloids Surf. A 320 (2008) 183–188.
[12] Th.F. Tadros, W. Liang, B. Costello, P.F. Luckham, Correlation of the rheology of concentrated dispersions with interparticle interactions, Colloids Surf. A 79 (1993) 105–114.
[13] M. Anpo, M. Takeuchi, The design and development of highly reactive titanium oxide photocatalysts operating under visible light irradiation, J. Catal. 216 (2003) 505–516.
[14] P. Santanu, C.K. Kartic, A review on experimental studies of surfactant adsorption at hydrophilic solid–water interface, Adv. Colloid Interface Sci. 110 (2004) 75–95.
[15] J. Duval, J. Lyklema, J.M. Kleijn, P.L. Herman, Amphifunctionally electrified interface: coupling of electronic and ionic surface-charging processes, Langmuir 17 (2001) 7573–7581.
[16] J. Lyklema, The bottom size of colloids, Bull. Pol. Acad.: Tech. 53 (2005) 317–323.
[17] J. Lyklema, Electrokinetics after Smoluchowski, Colloids Surf. A 222 (2003).
[18] S. Lu, R. Pugh, E. Forssberg, Interfacial Separation of Particles, Elsevier B.V., The Netherlands, 2005. pp. 172–240.
[19] S. Kim, W. Choi, Visible-light-induced photocatalytic degradation of 4-chlorophenol and phenolic compounds in aqueous suspension of pure titania: demonstrating the existence of surface-complex-mediated path, J. Phys. Chem. 109 (2005) 5243–5249.
[20] M. Diebold, The causes, The causes and prevention of titanium dioxide induced photodegradation of paints. Part I: theoretical considerations and durability, Surf. Coat. Int. 6 (1995) 250–256.
[21] T.A. Egerton, I.R. Tooley, Effect of changes in TiO_2 dispersion on its measured photocatalytic activity, J. Phys. Chem. B 108 (2004) 5066–5072.
[22] D.P. Colombo Jr., R.M. Bowman, Does interfacial charge transfer compete with charge carrier recombination? A femto second diffused reflectance investigation of TiO_2 nanoparticles, J. Phys. Chem. 100 (1996) 18445–18449.
[23] E. Ukaji, T. Furusawa, M. Sato, N. Suzuki, The effect of surface modification with silane coupling agent on suppressing the photo-catalytic activity of fine TiO_2 particles as inorganic UV filter, Appl. Surf. Sci. 254 (2007) 563–569.
[24] L.X. Chen, T. Rajh, Z. Wang, M.C. Thurnauer, XAFS studies of surface structure of TiO_2 nanoparticles and photocatalytic reduction of metal ions, J. Phys. Chem. B 101 (1997) 10688–10697.
[25] T. Tsuzuki, Abnormal transmittance of refractive index-modified ZnO organic hybrid films, Macromol. Mater. Eng. 293 (2008) 109–113.
[26] C. Lu, B. Yang, High refractive index organic–inorganic nanocomposite: design, synthesis, and application, J. Mater. Chem. 19 (2009) 2884–2901.
[27] S. Underwood, P. Mulvaney, Effect of the solution refractive index on the color of gold colloids, Langmuir 10 (1994) 3427–3430.
[28] K.L. Kelly, E. Coronado, L.L. Zhao, G.C. Schatz, The optical properties of metal nanoparticles: the influence of size, shape, and dielectric environment, J. Phys. Chem. B 107 (2003) 668–677.
[29] J.A. Creighton, D.G. Eadon, Ultraviolet–visible absorption spectra of the colloidal metallic elements, J. Chem. Soc., Faraday Trans. 87 (1991) 3881–3891.
[30] P. Mulvaney, Surface plasmon spectroscopy of nanosized metal particles, Langmuir 12 (1996) 788–800.
[31] H. Zhu, C. Tao, S. Zheng, S. Wu, J. Li, Effect of alkyl chain length on phase transfer of surfactant capped Au nanoparticles across the water/toluene interface, Colloids Surf., A 256 (2005) 17–20.

Please cite this article in press as: I.M. Joni et al., Decolorization of beads-milled TiO_2 nanoparticles suspension in an organic solvent, Advanced Powder Technology (2011), doi:10.1016/j.apt.2010.12.008